Supplementary Information

Two dominant self-assembly pathways to a Pd_3L_6 double-walled triangle

Tomoki Tateishi, Shumpei Kai, Yuya Sasaki, Tatsuo Kojima, Satoshi Takahashi and Shuichi Hiraoka*

Department of Basic Science, Graduate School of Arts and Sciences
The University of Tokyo
3-8-1 Komaba, Meguro-ku, Tokyo 153-8902, Japan
E-mail: chiraoka@mail.ecc.u-tokyo.ac.jp

Contents

General Information

^{1}H NMR spectra were recorded using a Bruker AV-500 (500 MHz) spectrometer. All ^{1}H spectra were referenced using a residual solvent peak, CD_3NO_2 (δ 4.33). Electrospray ionization time-of-flight (ESI-TOF) mass spectra were obtained using a Waters Xevo G2-S Tof mass spectrometer.

Materials

Unless otherwise noted, all solvents and reagents were obtained from commercial suppliers (TCI Co., Ltd., WAKO Pure Chemical Industries Ltd., KANTO Chemical Co., Inc., and Sigma-Aldrich Co.) and were used as received. CD_3NO_2 was purchased from Acros Organics and used after dehydration with Molecular Sieves 4Å. Ditopic ligand **1** [1] and $PdPy^*_4(BF_4)_2$ [2] were prepared according to the literature.

Monitoring of the Self-Assembly of DWT by ^{1}H NMR

Procedure for Monitoring the Self-Assembly Process of $Pd_3\mathbf{1}_6(BF_4)_6$ Double-Walled Triangle (DWT)

A 2.4 mM solution of [2.2]paracyclophane in $CHCl_3$ (125 μL), which was used as an internal standard, was added to two NMR tubes (tubes **I** and **II**) and the solvent was removed in vacuo. A solution of $PdPy^*_4(BF_4)_2$ (12 mM) in CD_3NO_2 was prepared (solution **A**). Solution **A** (50 μL) and CD_3NO_2 (450 μL) were added to tube **I**. The exact concentration of $PdPy^*_4(BF_4)_2$ in solution **A** was determined through the comparison of the signal intensity with [2.2]paracyclophane by ^{1}H NMR. A solution of ditopic ligand **1** (12 mM) in $CHCl_3$ (100 μL) was added to tube **II** and the solvent was removed in vacuo. Then CD_3NO_2 (500 μL) was added to tube **II** and the exact amount of **1** in tube **II** was determined through the comparison of the signal intensity with [2.2]paracyclophane by ^{1}H NMR. 0.50 eq. (against the amount of ligand **1** in tube **II**) of solution **A** (*ca.* 50 μL; the exact amount was determined based on the exact concentration of solution **A** and of ligand in tube **II**) were added to tube **II** at 263 K. The self-assembly of the $Pd_3\mathbf{1}_6(BF_4)_6$ (**DWT**) was monitored at 298 K by ^{1}H NMR spectroscopy. Examples of the ^{1}H NMR spectra are shown in Figures 2 and S1. The exact ratio of **1** and $PdPy^*_4(BF_4)_2$ was unambiguously determined by the comparison of the integral value of each ^{1}H signal of [2.2]paracyclophane. The amounts of **1**, $PdPy^*_4(BF_4)_2$, **DWT**, and Py* were quantified by the integral value of each ^{1}H signal against the signal of the internal standard ([2.2]paracyclophane). In order to confirm the reproducibility, the same experiment was carried out three times (runs 1–3) in total. These data, the average values of the existence ratios and the ($\langle n \rangle$, $\langle k \rangle$) values are listed in Tables S1–S5.

Determination of the Existence Ratios of Each Species

The relative integral value of each ^{1}H NMR signal against the internal standard [2.2]paracyclophane is used as the integral value in this description. We define the integral values of the signal for the substrates and the products at each time *t* as follows:

$I_L(t)$: 1/4 of the integral value of the *a* proton in free ligand **1**
$I_M(t)$: the integral value of the *h* proton of Py* in $[PdPy*_4]^{2+}$
$I_{\mathbf{DWT}}(t)$: 1/4 of the integral value of the *a* proton in the $Pd_3\mathbf{1}_6$ (**DWT**)
$I_{Py*}(t)$: the integral value of the *g* proton of free Py*

$I_M(0)$ was determined based on the exact concentration of solution **A** determined by ^{1}H NMR and the exact volume of solution **A** added into tube **II**.
$I_L(0)$ was determined by ^{1}H NMR measurement before the addition of solution **A** into tube **II**.

Existence ratio of $[PdPy*_4]^{2+}$

As the total amount of $[PdPy*_4]^{2+}$ corresponds to $I_M(0)$, the existence ratio of $[PdPy*_4]^{2+}$ at *t* is expressed by $I_M(t)/I_M(0)$.

Existence ratio of **1**

As the total amount of free ligand **1** corresponds to $I_L(0)$, the existence ratio of **1** at *t* is expressed by $I_L(t)/I_L(0)$.

Existence ratio of **DWT**

As the total amount of **DWT** is quantified based on **1**, the existence ratio of the **DWT** at *t* is expressed by $I_{\mathbf{DWT}}(t)/I_L(0)$.

Existence ratio of Py*

As the total amount of Py* corresponds to $I_M(0)$, the existence ratio of Py* at *t* is expressed by $I_{Py*}(t)/I_M(0)$.

Existence ratio of the total intermediates not observed by ^{1}H NMR (**Int**)

The existence ratio of the total intermediates not observed by ^{1}H NMR (**Int**) is determined based on the amount of ligand **1** in **Int**. Thus the existence ratio of **Int** is calculated by subtracting the other species containing **1** (free **1** and **DWT**) from the total amount of **1** ($I_L(0)$). The existence ratio of **Int** at *t* is expressed by $(I_L(0) - I_L(t) - I_{\mathbf{DWT}}(t))/I_L(0)$.

⟨*a*⟩

The total amount of Pd^{2+} ions corresponds to $I_M(0)/4$. The amount of Pd^{2+} ions in $[PdPy*_4]^{2+}$ at *t* corresponds to $I_M(t)/4$. The amount of Pd^{2+} ions in **DWT** at *t* corresponds to $I_{\mathbf{DWT}}(t)/2$. The amount of Pd^{2+} ions in **Int** at *t* is thus expressed by $I_M(0)/4 - I_M(t)/4 - I_{\mathbf{DWT}}(t)/2$.

⟨*b*⟩

The total amount of ligand **1** corresponds to $I_L(0)$. The amount of free ligand **1** at *t* corresponds to $I_L(t)$. The amounts of ligand **1** in **DWT** at *t* corresponds to $I_{\mathbf{DWT}}(t)$. The amount of ligand **1** in **Int** at *t* is thus expressed by $I_L(0) - I_L(t) - I_{\mathbf{DWT}}(t)$.

$\langle c \rangle$

The total amount of Py* corresponds to $I_M(0)$. The amount of free Py* at t corresponds to $I_{Py*}(t)$. The amount of Py* in $[PdPy*_4]^{2+}$ at t corresponds to $I_M(t)$. The amount of Py* in **Int** at t is thus expressed by $I_M(0) - I_{Py*}(t) - I_M(t)$.

The $\langle n \rangle$ and $\langle k \rangle$ values are determined with these $\langle a \rangle$, $\langle b \rangle$, and $\langle c \rangle$ values by eqs. (1) and (2).

$$\langle n \rangle = \frac{4\langle a \rangle - \langle c \rangle}{\langle b \rangle} \quad (1)$$

$$\langle k \rangle = \frac{\langle a \rangle}{\langle b \rangle} \quad (2)$$

^{1}H NMR Spectra for the Self-Assembly of DWT from 1 and PdPy*$_4$(BF$_4$)$_2$ in CD_3NO_2

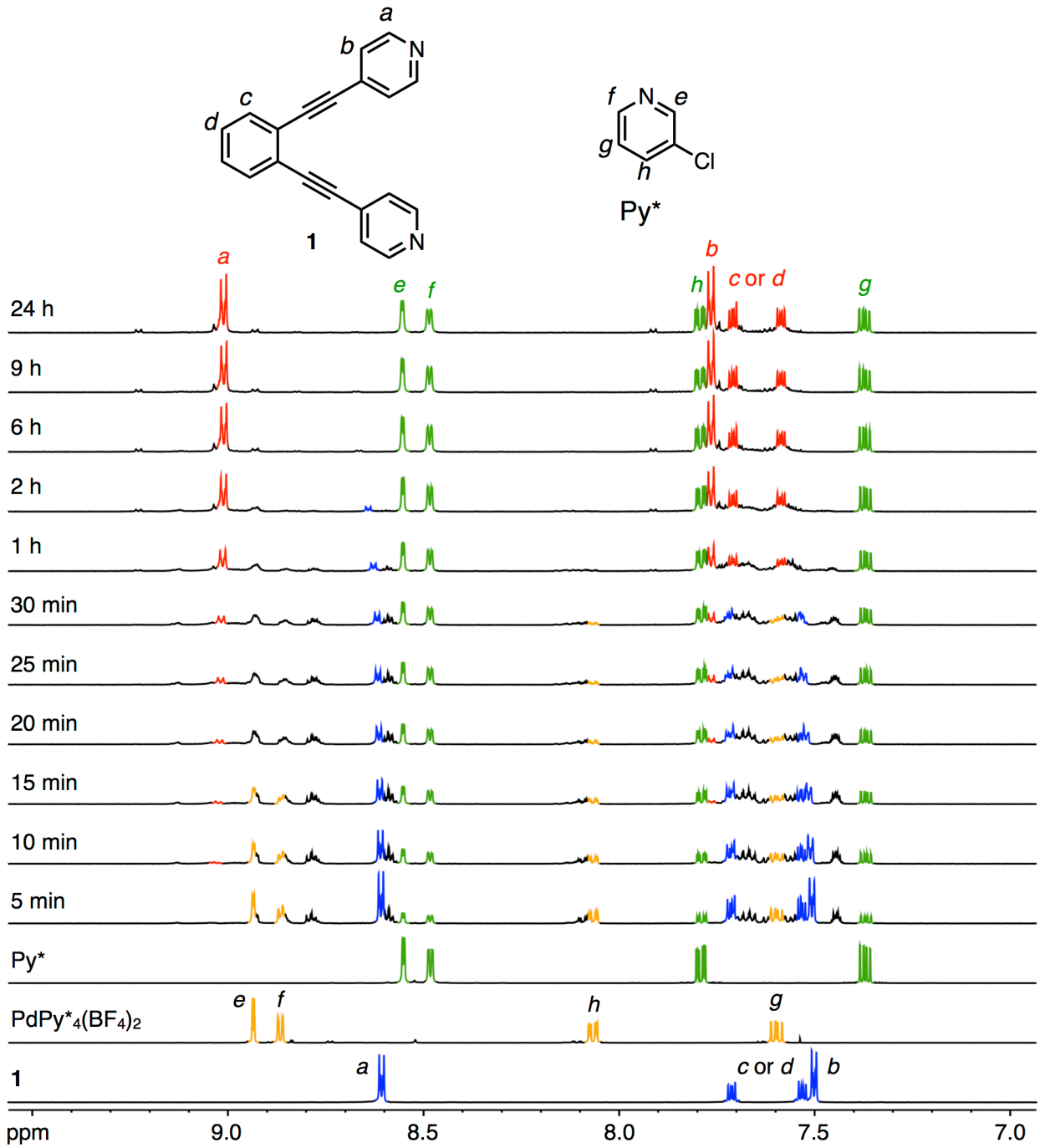

Figure S1. ^{1}H NMR spectra (500 MHz, CD_3NO_2, 298 K, aromatic region) of the reaction mixture for the self-assembly of **DWT** from **1** and PdPy*$_4$(BF$_4$)$_2$ at 298 K ([**1**]$_0$ = 1.6 mM). The signals colored in blue, orange, red, and green indicate free **1**, PdPy*$_4$(BF$_4$)$_2$, **DWT**, and Py*, respectively.

Time Variation of 1, $PdPy^*_4(BF_4)_2$, DWT, Py*, Int, and the ($\langle n \rangle$, $\langle k \rangle$) Values for the Self-Assembly of DWT

Table S1. Average time variation of **1**, $PdPy^*_4(BF_4)_2$, **DWT**, Py*; $\langle a \rangle$–$\langle c \rangle$ values of the average composition of the intermediates ($Pd_{\langle a \rangle}\mathbf{1}_{\langle b \rangle}Py^*_{\langle c \rangle}$); ($\langle n \rangle$, $\langle k \rangle$) values for the self-assembly of **DWT** from **1** and $PdPy^*_4(BF_4)_2$ in CD_3NO_2 at 298 K ($[\mathbf{1}]_0$ = 1.6 mM).

Time / min	**1** / %	$[PdPy^*_4]^{2+}$ / %	**DWT** / %	Py* / %	**Int** / %	$\langle a \rangle$	$\langle b \rangle$	$\langle c \rangle$	$\langle n \rangle$	$\langle k \rangle$
0	100	100	0.0	0.0	0.0	—	—	—	—	—
5	40.1	41.3	0.0	36.9	59.9	0.105	0.214	0.156	1.227	0.489
10	26.1	23.0	6.2	50.7	67.7	0.127	0.242	0.188	1.315	0.523
15	19.9	15.3	8.8	60.5	71.3	0.136	0.255	0.174	1.451	0.533
20	17.1	10.7	14.0	66.6	68.9	0.134	0.246	0.162	1.531	0.547
25	13.3	8.3	18.5	71.1	68.2	0.131	0.244	0.148	1.551	0.538
30	11.3	6.5	23.8	75.3	65.0	0.125	0.232	0.130	1.599	0.538
35	10.5	5.5	28.8	77.9	60.7	0.117	0.217	0.119	1.630	0.543
40	10.0	5.0	32.1	80.2	57.9	0.112	0.207	0.107	1.672	0.544
45	9.6	4.1	35.3	82.5	55.2	0.108	0.197	0.096	1.727	0.551
50	8.8	3.4	38.8	84.1	52.4	0.103	0.188	0.090	1.744	0.553
55	8.5	3.0	40.5	85.2	51.0	0.101	0.182	0.084	1.770	0.555
60	7.4	2.7	42.5	86.2	50.2	0.098	0.180	0.080	1.758	0.548
120	4.7	0.0	53.1	92.9	42.3	0.084	0.151	0.051	1.886	0.555
180	3.6	0.0	59.9	94.8	36.5	0.072	0.131	0.037	1.914	0.549
240	3.4	0.0	61.2	95.6	35.4	0.069	0.127	0.031	1.946	0.549
300	2.9	0.0	62.7	96.1	34.4	0.067	0.123	0.028	1.946	0.543
360	2.9	0.0	64.2	96.2	33.0	0.064	0.118	0.027	1.941	0.544
420	2.7	0.0	64.6	96.4	32.7	0.063	0.117	0.026	1.947	0.542
480	2.6	0.0	65.6	96.7	31.8	0.061	0.114	0.023	1.962	0.543
540	0.0	0.0	66.3	96.8	33.7	0.060	0.121	0.023	1.812	0.500
720	0.0	0.0	68.7	97.3	31.3	0.056	0.112	0.019	1.827	0.500
1440	0.0	0.0	73.4	97.6	26.6	0.048	0.095	0.017	1.819	0.500

Table S2. Standard errors for each time point of **1**, $PdPy*_4(BF_4)_2$, **DWT**, Py*; $\langle a\rangle$–$\langle c\rangle$ values of the average composition of the intermediates ($Pd_{\langle a\rangle}\mathbf{1}_{\langle b\rangle}Py*_{\langle c\rangle}$); ($\langle n\rangle$, $\langle k\rangle$) values for the self-assembly of **DWT** from **1** and $PdPy*_4(BF_4)_2$ in CD_3NO_2 at 298 K ($[\mathbf{1}]_0$ = 1.6 mM).

Time / min	**1** / %	$[PdPy*_4]^{2+}$ / %	**DWT** / %	Py* / %	**Int** / %	$\langle a\rangle$	$\langle b\rangle$	$\langle c\rangle$	$\langle n\rangle$	$\langle k\rangle$
0	0.0	0.0	0.0	0.0	0.0	—	—	—	—	—
5	0.91	4.92	0.00	4.34	0.91	0.009	0.003	0.024	0.128	0.036
10	2.24	3.73	2.18	5.20	0.20	0.002	0.003	0.012	0.100	0.014
15	2.12	3.58	3.43	5.63	1.33	0.004	0.005	0.016	0.122	0.019
20	1.28	3.04	3.80	5.11	2.58	0.005	0.010	0.016	0.120	0.021
25	0.79	2.29	3.89	5.12	3.24	0.005	0.013	0.022	0.121	0.017
30	0.27	2.33	3.60	5.08	3.35	0.004	0.013	0.021	0.125	0.018
35	0.58	1.90	4.39	4.73	3.90	0.006	0.015	0.021	0.110	0.013
40	0.85	1.64	4.34	4.68	3.59	0.006	0.014	0.023	0.108	0.009
45	0.74	1.41	4.74	4.04	4.07	0.007	0.016	0.020	0.095	0.009
50	0.82	1.40	5.37	3.85	4.62	0.008	0.018	0.019	0.090	0.010
55	0.72	1.38	4.83	3.91	4.21	0.007	0.017	0.019	0.106	0.012
60	0.64	1.18	5.13	3.50	4.52	0.008	0.018	0.018	0.091	0.010
120	0.48	0.00	2.30	1.53	1.93	0.004	0.007	0.011	0.071	0.004
180	0.83	0.00	1.66	0.81	1.57	0.003	0.007	0.006	0.047	0.012
240	0.95	0.00	1.20	0.86	0.99	0.002	0.005	0.006	0.033	0.014
300	1.10	0.00	0.95	0.72	0.60	0.001	0.003	0.005	0.024	0.017
360	1.13	0.00	0.66	0.73	0.56	0.000	0.003	0.005	0.027	0.018
420	1.17	0.00	0.76	0.73	0.62	0.001	0.003	0.005	0.028	0.019
480	1.21	0.00	0.25	0.72	0.97	0.000	0.005	0.005	0.033	0.021
540	0.00	0.00	0.51	0.73	0.51	0.000	0.001	0.005	0.040	0.000
720	0.00	0.00	0.16	0.82	0.16	0.001	0.001	0.006	0.052	0.000
1440	0.00	0.00	0.61	0.75	0.61	0.001	0.002	0.005	0.053	0.000

Table S3. Time variation of **1**, $PdPy*_4(BF_4)_2$, **DWT**, Py*; ⟨*a*⟩–⟨*c*⟩ values of the average composition of the intermediates ($Pd_{\langle a\rangle}\mathbf{1}_{\langle b\rangle}Py*_{\langle c\rangle}$); (⟨*n*⟩, ⟨*k*⟩) values for the self-assembly of **DWT** from **1** and $PdPy*_4(BF_4)_2$ in CD_3NO_2 at 298 K ($[\mathbf{1}]_0$ = 1.6 mM). (run 1)

Time / min	**1** / %	$[PdPy*_4]^{2+}$ / %	**DWT** / %	Py* / %	**Int** / %	⟨*a*⟩	⟨*b*⟩	⟨*c*⟩	⟨*n*⟩	⟨*k*⟩
0	100	100	0.0	0.0	0.0	—	—	—	—	—
5	41.9	47.4	0.0	28.4	58.1	0.095	0.210	0.175	0.978	0.453
10	29.8	30.3	2.3	40.3	67.8	0.122	0.246	0.213	1.121	0.497
15	22.9	22.4	4.4	49.2	72.7	0.132	0.263	0.205	1.232	0.503
20	18.7	16.6	7.9	56.5	73.4	0.137	0.266	0.195	1.322	0.514
25	14.3	12.7	11.3	61.0	74.4	0.138	0.269	0.190	1.336	0.511
30	11.7	10.8	16.7	65.3	71.6	0.131	0.259	0.173	1.359	0.506
35	11.6	9.0	20.0	68.8	68.4	0.128	0.248	0.161	1.426	0.519
40	11.5	7.8	23.5	71.1	65.0	0.124	0.235	0.153	1.464	0.528
45	10.8	6.6	26.0	74.7	63.2	0.122	0.229	0.135	1.540	0.533
50	10.1	5.9	28.6	76.6	61.3	0.119	0.222	0.127	1.566	0.534
55	9.3	5.5	31.8	77.7	58.9	0.113	0.213	0.121	1.562	0.532
60	8.3	4.7	33.3	79.4	58.4	0.112	0.212	0.115	1.578	0.530
120	4.7	0.0	50.3	89.8	45.0	0.090	0.163	0.074	1.756	0.552
180	3.3	0.0	57.0	93.4	39.7	0.078	0.144	0.048	1.832	0.541
240	3.3	0.0	59.4	94.6	37.3	0.074	0.135	0.039	1.886	0.544
300	2.3	0.0	62.2	96.2	35.5	0.069	0.129	0.028	1.916	0.533
360	2.3	0.0	64.9	96.2	32.8	0.064	0.119	0.027	1.910	0.535
420	1.9	0.0	65.7	96.7	32.4	0.062	0.117	0.024	1.912	0.529
480	1.6	0.0	65.7	97.1	32.7	0.062	0.118	0.021	1.920	0.524
540	0.0	0.0	67.0	97.3	33.0	0.060	0.120	0.020	1.837	0.500
720	0.0	0.0	68.5	98.1	31.5	0.057	0.114	0.014	1.877	0.500
1440	0.0	0.0	74.6	98.3	25.4	0.046	0.092	0.012	1.870	0.500

Table S4. Time variation of **1**, $PdPy*_4(BF_4)_2$, **DWT**, Py*; ⟨*a*⟩–⟨*c*⟩ values of the average composition of the intermediates ($Pd_{\langle a\rangle}\mathbf{1}_{\langle b\rangle}Py*_{\langle c\rangle}$); (⟨*n*⟩, ⟨*k*⟩) values for the self-assembly of **DWT** from **1** and $PdPy*_4(BF_4)_2$ in CD_3NO_2 at 298 K ($[\mathbf{1}]_0$ = 1.5 mM). (run 2)

Time / min	**1** / %	$[PdPy*_4]^{2+}$ / %	**DWT** / %	Py* / %	**Int** / %	⟨*a*⟩	⟨*b*⟩	⟨*c*⟩	⟨*n*⟩	⟨*k*⟩
0	100	100	0.0	0.0	0.0	—	—	—	—	—
5	39.3	45.0	0.0	39.5	60.7	0.096	0.213	0.109	1.300	0.453
10	26.3	20.3	6.4	55.3	67.4	0.128	0.236	0.171	1.452	0.544
15	21.1	11.2	6.4	66.3	72.5	0.144	0.254	0.158	1.653	0.569
20	18.1	6.4	13.0	72.9	68.8	0.141	0.241	0.145	1.740	0.585
25	14.0	4.9	19.4	77.8	66.6	0.132	0.233	0.121	1.753	0.568
30	11.3	2.8	26.1	81.8	62.6	0.124	0.219	0.108	1.780	0.568
35	9.6	2.5	32.6	84.7	57.8	0.114	0.202	0.090	1.803	0.561
40	8.5	2.1	36.9	86.7	54.6	0.107	0.191	0.078	1.824	0.559
45	8.2	1.8	41.4	88.1	50.3	0.099	0.176	0.071	1.853	0.564
50	7.3	1.0	46.9	89.4	45.9	0.091	0.161	0.067	1.856	0.568
55	7.1	0.8	48.4	91.0	44.5	0.089	0.156	0.058	1.912	0.570
60	6.1	0.6	51.0	91.1	42.9	0.085	0.150	0.058	1.871	0.564
120	5.5	0.0	51.3	94.5	43.2	0.085	0.151	0.038	1.999	0.563
180	5.1	0.0	59.9	94.8	35.0	0.070	0.123	0.037	1.995	0.573
240	5.1	0.0	60.7	94.9	34.1	0.069	0.120	0.036	2.000	0.575
300	5.0	0.0	61.4	94.9	33.5	0.068	0.117	0.036	1.994	0.575
360	5.0	0.0	62.9	94.9	32.1	0.065	0.112	0.036	1.994	0.579
420	5.0	0.0	63.1	95.0	31.8	0.065	0.111	0.035	2.003	0.579
480	5.0	0.0	65.1	95.4	29.8	0.061	0.104	0.032	2.027	0.585
540	0.0	0.0	65.3	95.4	34.7	0.061	0.122	0.032	1.734	0.500
720	0.0	0.0	68.6	95.6	31.4	0.055	0.110	0.030	1.722	0.500
1440	0.0	0.0	72.7	96.1	27.3	0.048	0.096	0.028	1.712	0.500

Table S5. Time variation of **1**, $PdPy*_4(BF_4)_2$, **DWT**, Py*; ⟨*a*⟩–⟨*c*⟩ values of the average composition of the intermediates ($Pd_{\langle a\rangle}\mathbf{1}_{\langle b\rangle}Py*_{\langle c\rangle}$); (⟨*n*⟩, ⟨*k*⟩) values for the self-assembly of **DWT** from **1** and $PdPy*_4(BF_4)_2$ in CD_3NO_2 at 298 K ($[\mathbf{1}]_0$ = 1.6 mM). (run 3)

Time / min	**1** / %	$[PdPy*_4]^{2+}$ / %	**DWT** / %	Py* / %	**Int** / %	⟨*a*⟩	⟨*b*⟩	⟨*c*⟩	⟨*n*⟩	⟨*k*⟩
0	100	100	0.0	0.0	0.0	—	—	—	—	—
5	39.0	31.6	0.0	42.8	61.0	0.123	0.220	0.184	1.404	0.561
10	22.1	18.2	9.9	56.5	68.0	0.129	0.245	0.182	1.372	0.528
15	15.8	12.2	15.6	65.9	68.6	0.130	0.247	0.157	1.469	0.527
20	14.6	9.2	21.0	70.3	64.4	0.126	0.232	0.147	1.532	0.542
25	11.8	7.4	24.7	74.4	63.5	0.122	0.229	0.131	1.565	0.535
30	10.8	5.9	28.5	78.9	60.8	0.118	0.219	0.109	1.659	0.540
35	10.4	5.0	33.8	80.1	55.8	0.110	0.201	0.107	1.662	0.549
40	9.9	4.9	36.1	82.7	54.0	0.106	0.194	0.089	1.728	0.546
45	9.7	3.9	38.5	84.9	51.9	0.104	0.187	0.081	1.789	0.556
50	9.1	3.4	40.8	86.2	50.1	0.100	0.180	0.075	1.811	0.557
55	9.1	2.8	41.4	86.9	49.6	0.100	0.178	0.075	1.835	0.563
60	7.7	2.8	43.2	88.0	49.1	0.097	0.177	0.066	1.824	0.550
120	3.8	0.0	57.6	94.3	38.5	0.076	0.139	0.041	1.902	0.550
180	2.3	0.0	62.8	96.2	34.9	0.067	0.126	0.027	1.916	0.533
240	1.9	0.0	63.5	97.3	34.7	0.066	0.125	0.019	1.952	0.527
300	1.4	0.0	64.6	97.4	34.0	0.064	0.123	0.019	1.926	0.520
360	1.3	0.0	64.7	97.4	34.0	0.064	0.123	0.019	1.920	0.518
420	1.3	0.0	64.9	97.5	33.9	0.063	0.122	0.018	1.926	0.518
480	1.3	0.0	66.0	97.8	32.8	0.061	0.118	0.016	1.940	0.519
540	0.0	0.0	66.5	97.8	33.5	0.060	0.121	0.016	1.866	0.500
720	0.0	0.0	69.0	98.1	31.0	0.056	0.112	0.013	1.880	0.500
1440	0.0	0.0	72.8	98.3	27.2	0.049	0.098	0.012	1.875	0.500

Characterization of DWT

ESI-TOF Mass Spectrometry

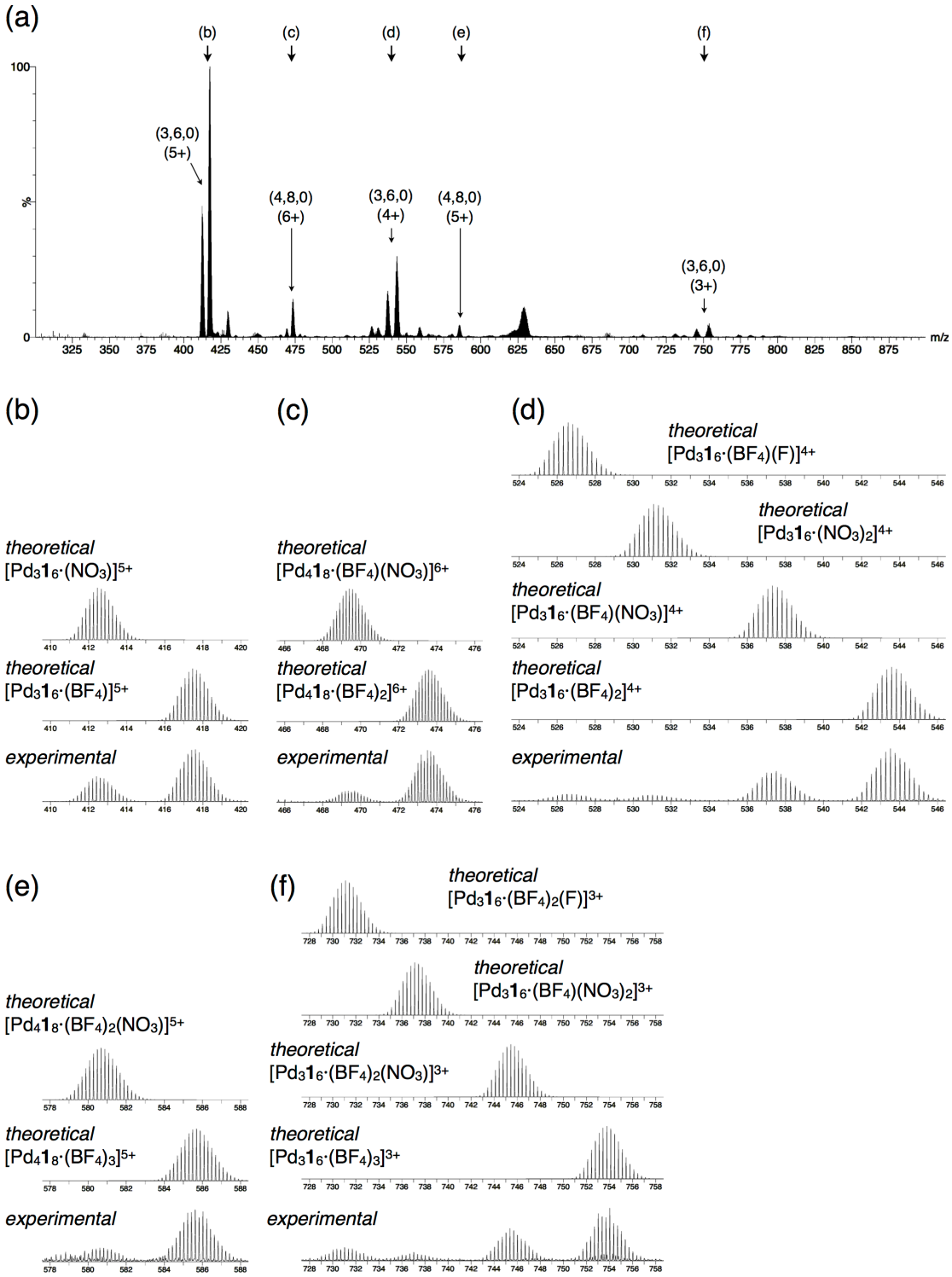

Figure S2. ESI-TOF mass spectra of the reaction mixture for the self-assembly of **DWT** from **1** and $PdPy^*_4(BF_4)_2$ in CD_3NO_2 at 298 K ($[\mathbf{1}]_0$ = 1.6 mM) recorded after convergence. Measurement condition: Capillary / 1.5 kV; Sampling Cone / 30 V; Source Offset / 80 V; Source / 80 °C; Desolvation / 150 °C; Cone Gas / 50 L h^{-1}; Desolvation Gas / 800 L h^{-1}. (a) *m/z*: 300–900, (b) $[Pd_3\mathbf{1}_6\cdot(NO_3)]^{5+}$ and $[Pd_3\mathbf{1}_6\cdot(BF_4)]^{5+}$, (c) $[Pd_4\mathbf{1}_8\cdot(BF_4)(NO_3)]^{6+}$ and $[Pd_4\mathbf{1}_8\cdot(BF_4)_2]^{6+}$, (d) $[Pd_3\mathbf{1}_6\cdot(BF_4)(F)]^{4+}$, $[Pd_3\mathbf{1}_6\cdot(NO_3)_2]^{4+}$, $[Pd_3\mathbf{1}_6\cdot(BF_4)(NO_3)]^{4+}$ and $[Pd_3\mathbf{1}_6\cdot(BF_4)_2]^{4+}$, (e) $[Pd_4\mathbf{1}_8\cdot(BF_4)_2(NO_3)]^{5+}$ and $[Pd_4\mathbf{1}_8\cdot(BF_4)_3]^{5+}$ and (f) $[Pd_3\mathbf{1}_6\cdot(BF_4)_2(F)]^{3+}$, $[Pd_3\mathbf{1}_6\cdot(BF_4)(NO_3)_2]^{3+}$, $[Pd_3\mathbf{1}_6\cdot(BF_4)_2(NO_3)]^{3+}$ and $[Pd_3\mathbf{1}_6\cdot(BF_4)_3]^{3+}$. (*a*, *b*, *c*) indicates species $Pd_a\mathbf{1}_bPy^*_c$.

^{1}H DOSY NMR Spectroscopy

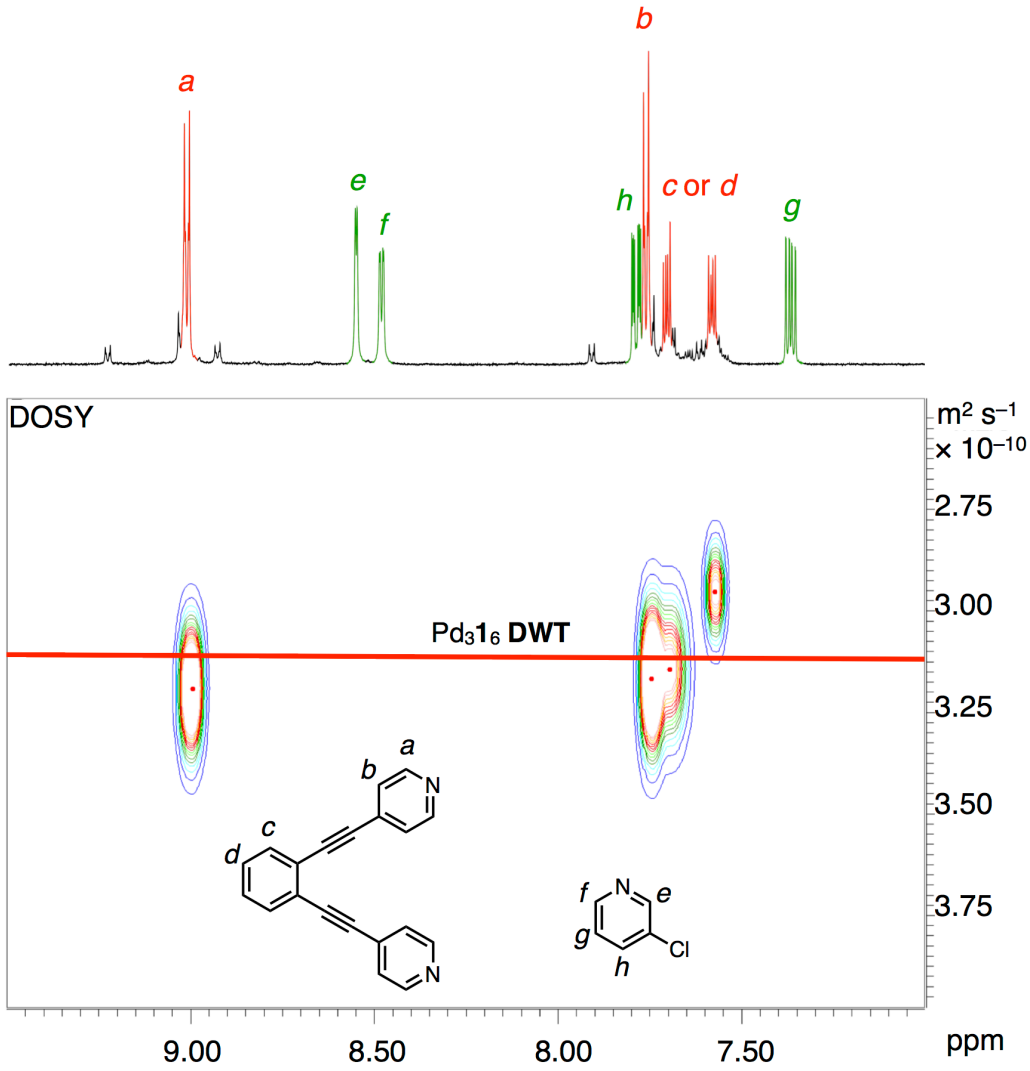

Figure S3. ^{1}H DOSY NMR spectrum (500 MHz, CD_3NO_2, 298 K, aromatic region) of the reaction mixture for the self-assembly of **DWT** from **1** and $PdPy^*_4(BF_4)_2$ at 298 K ($[\mathbf{1}]_0$ = 1.6 mM) recorded after convergence. Signals colored in red and green indicate **DWT** and Py*, respectively.

Table S6. A list of diffusion coefficients (D), errors, log$D$, and errors for log$D$ of **DWT**.

Peak	F2 / ppm	D / m^2 s^{-1}	Error	log$D$	error for log$D$
a	8.994	3.21×10^{-10}	1.04×10^{-11}	–9.493	0.032
b	7.745	3.19×10^{-10}	1.15×10^{-11}	–9.496	0.036
c or *d*	7.696	3.17×10^{-10}	1.12×10^{-11}	–9.499	0.035
c or *d*	7.573	2.98×10^{-10}	7.74×10^{-12}	–9.526	0.026
Avg.		3.14×10^{-10}	1.02×10^{-11}	–9.503	0.032

Table S7. A list of diffusion coefficients of **DWT** and double-walled square (**DWS**).

Substance	Solvent	D / m^2 s^{-1}	log D	Error	Hydrodynamic radius / Å
Pd_3**1**$_6$ **DWT** [1]	CD_3CN	5.0×10^{-10}	–9.3	—	12.8
Pd_4**1**$_8$ **DWS** [1]	DMSO-d_6	6.3×10^{-11}	–10.2	—	17.3
Pd_3**1**$_6$ **DWT**	CD_3NO_2	3.14×10^{-10}	–9.50	1.02×10^{-11}	11.4

Monitoring of the Self-Assembly of DWT by ESI-TOF Mass Spectrometry

A 1.76 mM solution of **1** in CD_3NO_2 (500 μL, 0.88 μmol) and a 8.8 mM solution of $PdPy^*_4(BF_4)_2$ in CD_3NO_2 (50 μL, 0.44 μmol) were mixed. At each time point, 50 μL of the reaction mixture was taken, diluted with CH_3NO_2 (450 μL), filtered through a membrane filter (pore size: 0.20 μm) and injected in the mass spectrometer with 5.0 μL/min flow rate to obtain ESI-TOF mass spectra (Figure S4). A list of predominantly observed species is shown in Table 1.

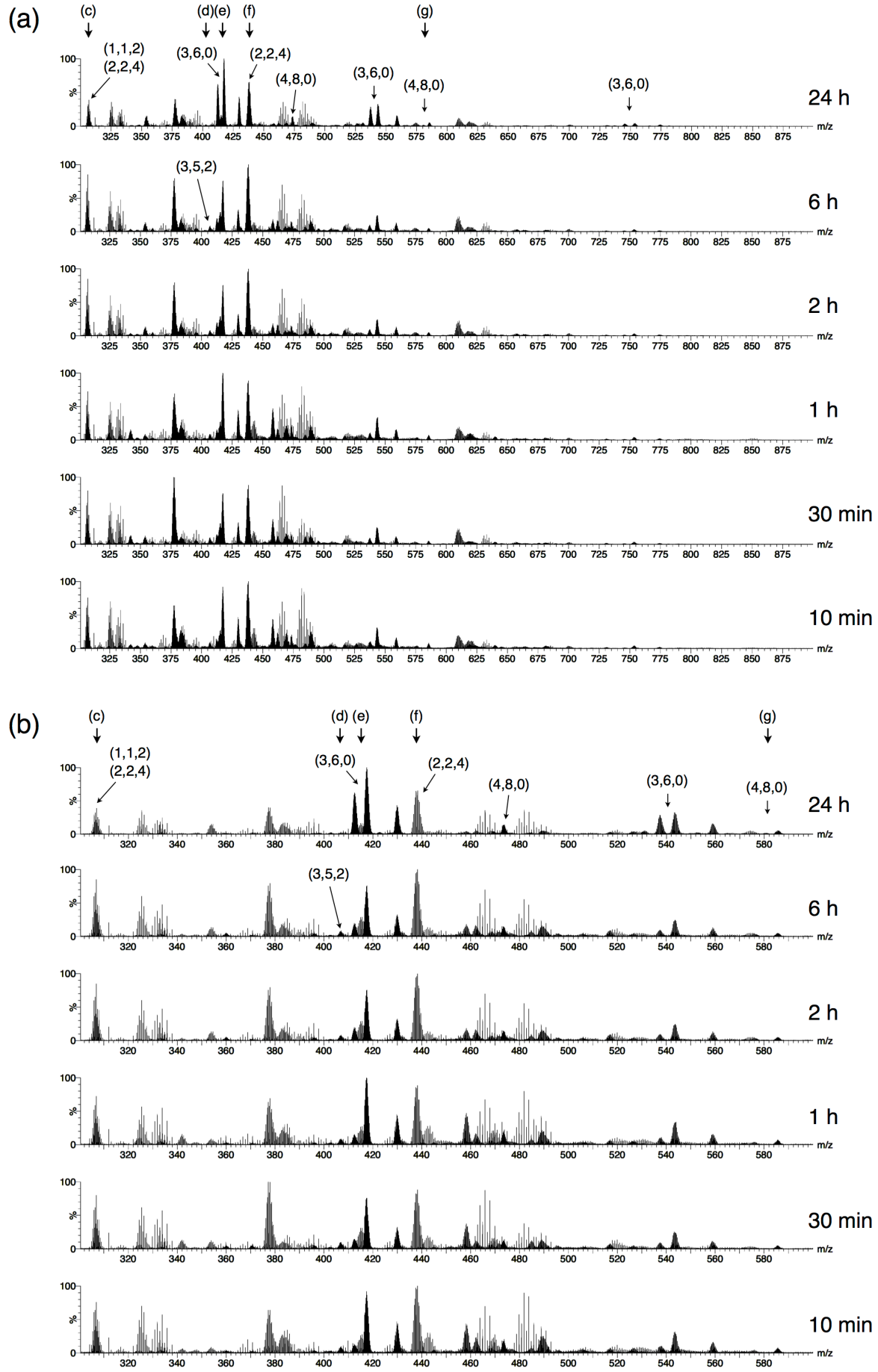
(a)
(c)
(d)(e)
(f)
(g)
(1,1,2)
(2,2,4)
(3,6,0)
(2,2,4)
(4,8,0)
(3,6,0)
(4,8,0)
(3,6,0)
24 h
(3,5,2)
6 h
2 h
1 h
30 min
10 min
%
m/z
(b)
(c)
(d) (e)
(f)
(g)
(1,1,2)
(2,2,4)
(3,6,0)
(2,2,4)
(4,8,0)
(3,6,0)
(4,8,0)
24 h
(3,5,2)
6 h
2 h
1 h
30 min
10 min

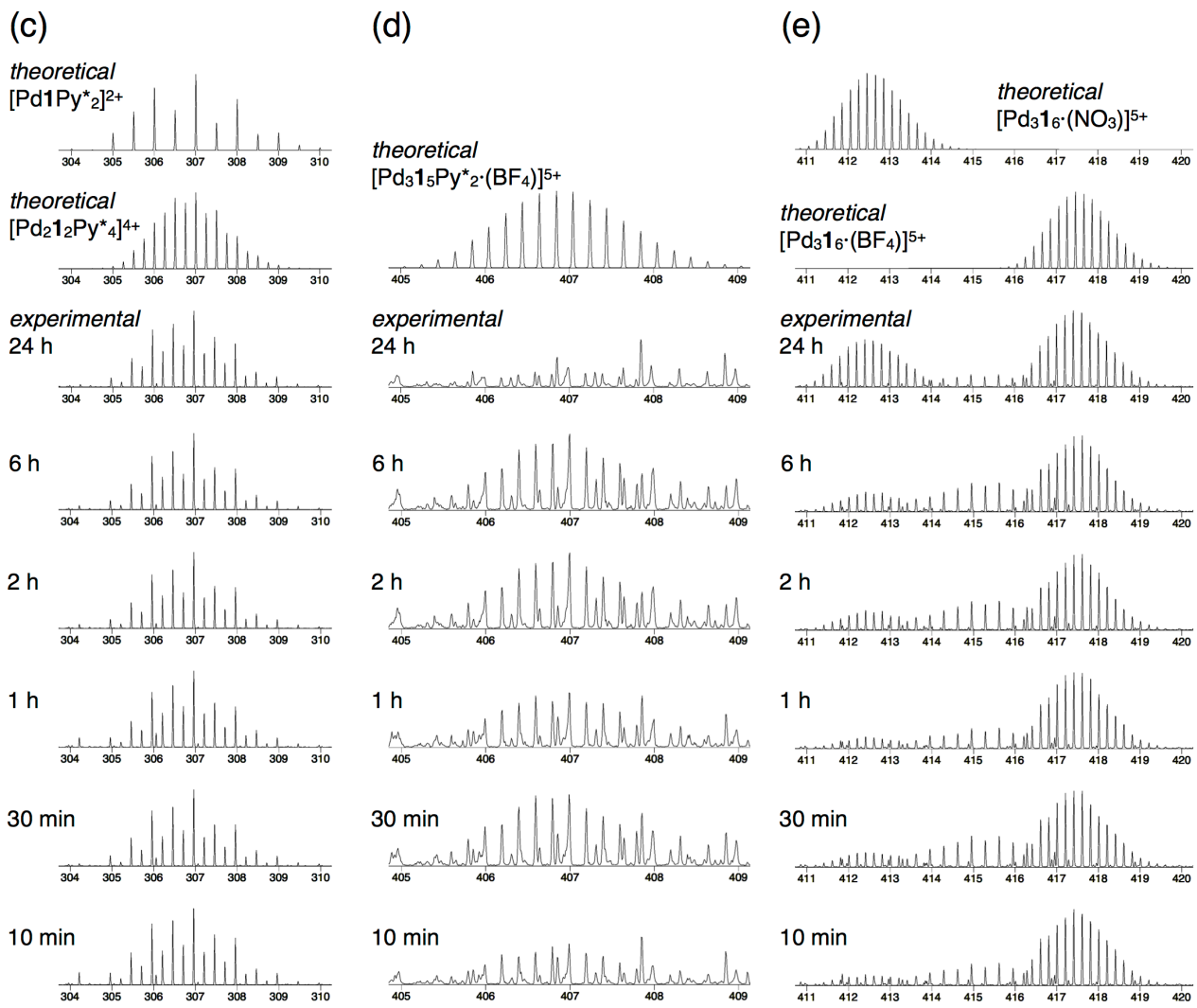
(c)
theoretical
[Pd1Py*2]2+
304 305 306 307 308 309 310
theoretical
[Pd21 2Py*4]4+
304 305 306 307 308 309 310
experimental
24 h
304 305 306 307 308 309 310
6 h
304 305 306 307 308 309 310
2 h
304 305 306 307 308 309 310
1 h
304 305 306 307 308 309 310
30 min
304 305 306 307 308 309 310
10 min
304 305 306 307 308 309 310
(d)
theoretical
[Pd3 1 5Py*2·(BF4)]5+
405 406 407 408 409
experimental
24 h
405 406 407 408 409
6 h
405 406 407 408 409
2 h
405 406 407 408 409
1 h
405 406 407 408 409
30 min
405 406 407 408 409
10 min
405 406 407 408 409
(e)
theoretical
[Pd3 1 6·(NO3)]5+
411 412 413 414 415 416 417 418 419 420
theoretical
[Pd3 1 6·(BF4)]5+
411 412 413 414 415 416 417 418 419 420
experimental
24 h
411 412 413 414 415 416 417 418 419 420
6 h
411 412 413 414 415 416 417 418 419 420
2 h
411 412 413 414 415 416 417 418 419 420
1 h
411 412 413 414 415 416 417 418 419 420
30 min
411 412 413 414 415 416 417 418 419 420
10 min
411 412 413 414 415 416 417 418 419 420

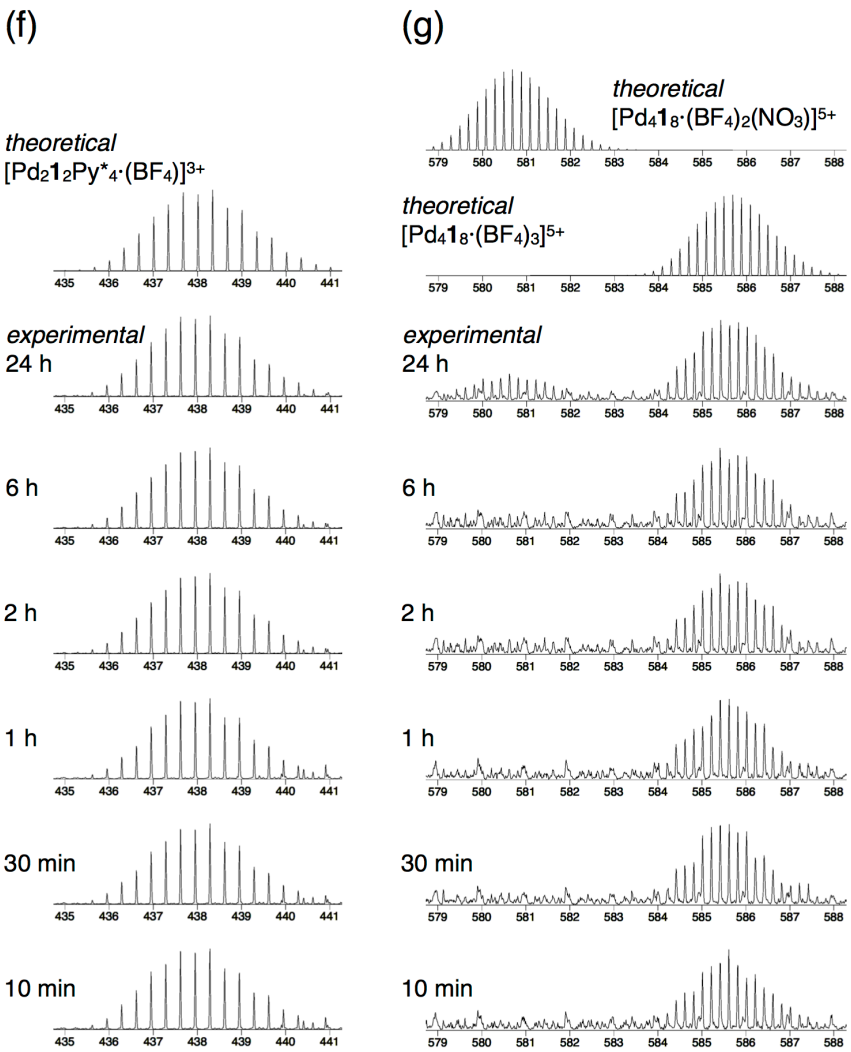

Figure S4. ESI-TOF mass spectra of the reaction mixture for the self-assembly of **DWT** from **1** and $PdPy^*_4(BF_4)_2$ in CD_3NO_2 at 298 K ($[\mathbf{1}]_0$ = 1.6 mM), measured at 10 min, 30 min, 1 h, 2 h, 6 h, and 24 h. Measurement condition: Capillary / 1.5 kV; Sampling Cone / 30 V; Source Offset / 80 V; Source / 40 °C; Desolvation / 40 °C; Cone Gas / 50 L h^{-1}; Desolvation Gas / 800 L h^{-1}. (a) *m/z*: 300–900, (b) *m/z*: 300–600, (c) $[Pd\mathbf{1}Py^*_2]^{2+}$ and $[Pd_2\mathbf{1}_2Py^*_4]^{4+}$, (d) $[Pd_3\mathbf{1}_5Py^*_2\cdot(BF_4)]^{5+}$, (e) $[Pd_3\mathbf{1}_6\cdot(NO_3)]^{5+}$ and $[Pd_3\mathbf{1}_6\cdot(BF_4)]^{5+}$, (f) $[Pd_2\mathbf{1}_2Py^*_4\cdot(BF_4)]^{3+}$ and (g) $[Pd_4\mathbf{1}_8\cdot(BF_4)_2(NO_3)]^{5+}$ and $[Pd_4\mathbf{1}_8\cdot(BF_4)_3]^{5+}$. (*a*, *b*, *c*) indicates species $Pd_a\mathbf{1}_bPy^*_c$.

Molecular Modeling Study of $[Pd_2\mathbf{1}_3Py^*_2]^{4+}$

Geometry optimization for $[Pd_2\mathbf{1}_3Py^*_2]^{4+}$ was performed by molecular mechanics (*MM*) calculation with Universal Force field (BIOVIA Material Studio 2017 R2, Accelrys Software Inc.).

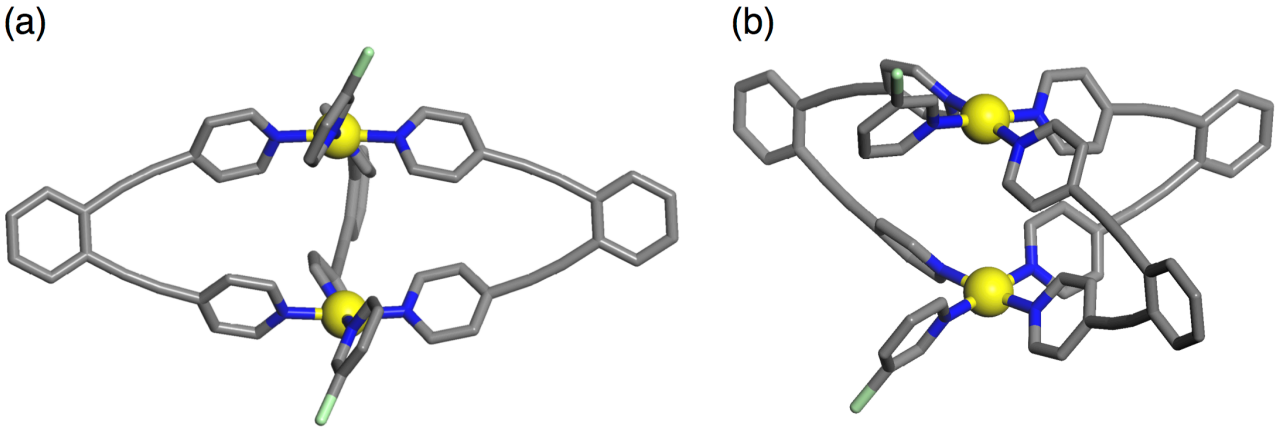

Figure S5. Optimized structures of $[Pd_2\mathbf{1}_3Py^*_2]^{4+}$ by *MM* calculation. Hydrogen atoms are omitted for clarity. Color labels: yellow, Pd; grey, C; blue, N; and light green, Cl. (a) and (b) indicate different views.

Possible Structures of (Pd, 1, Py*) = (2, 4, 3), (3, 5, 5), and (3, 6, 4)

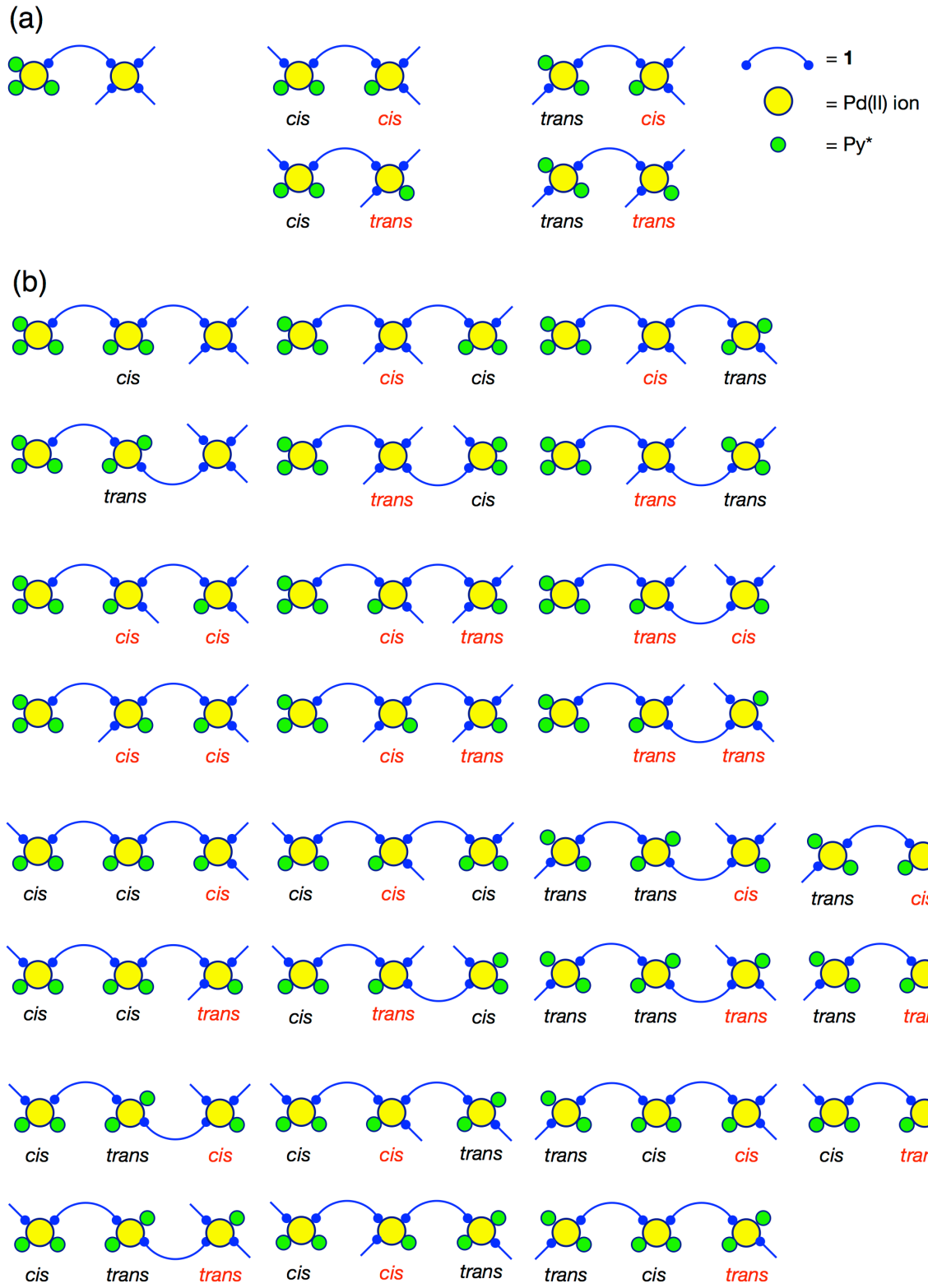

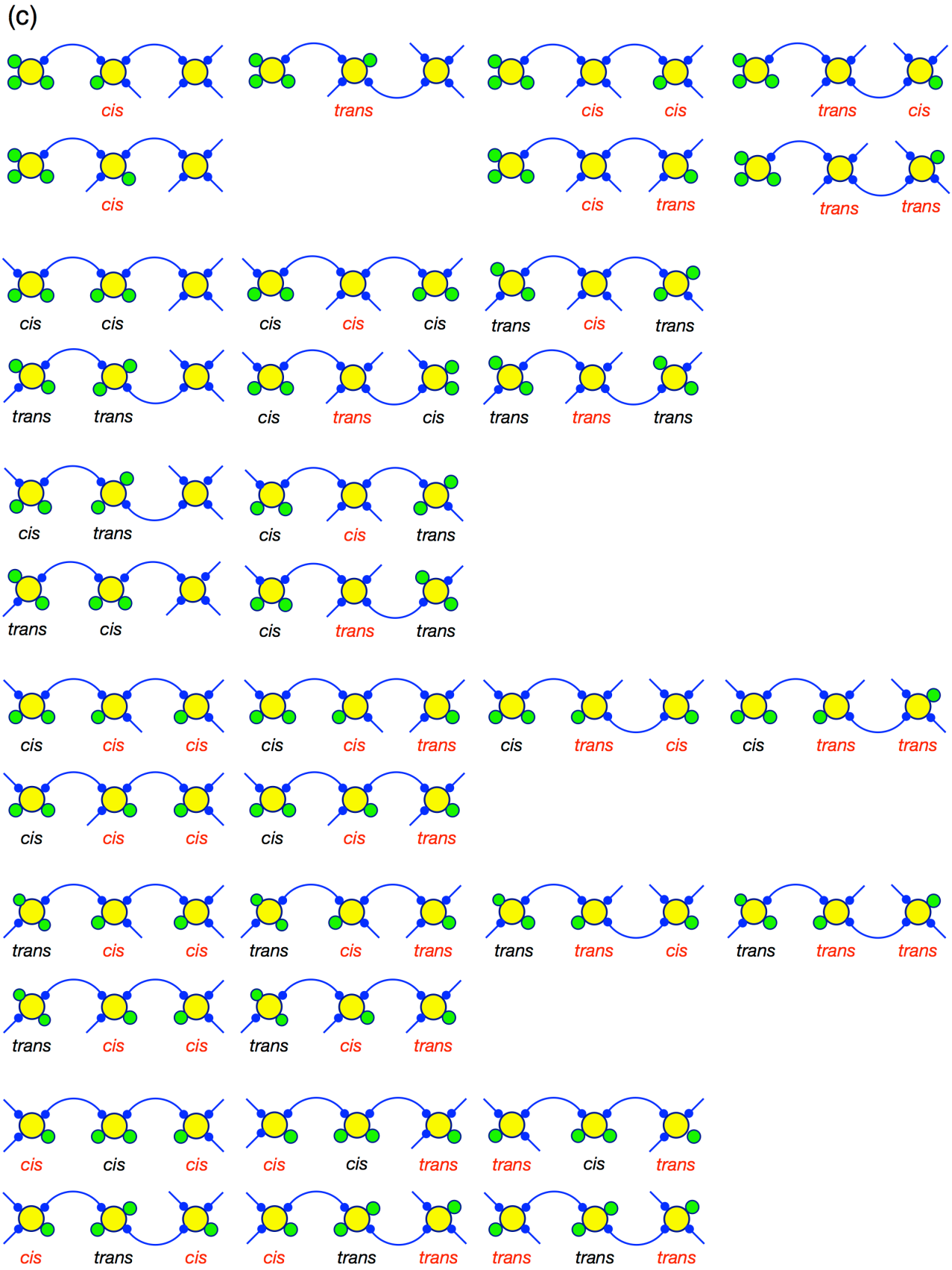

Figure S6. Possible structures of (a) (2, 4, 3), (b) (3, 5, 5), and (c) (3, 6, 4). (*a*, *b*, *c*) indicates species $Pd_a\mathbf{1}_bPy^*_c$. *cis* and *trans* colored in black indicate *cis* and *trans* configuration of Pd(II) centers possessing two Py* molecules, respectively and those in red indicate *cis* and *trans* configuration of Pd(II) centers possessing one or zero Py* molecule.

References

(1) K. Suzuki, M. Kawano and M. Fujita, *Angew. Chem. Int. Ed.*, 2007, **46**, 2819–2822.

(2) T. Tateishi, W. Zhu, L. H. Foianesi-Takeshige, T. Kojima, K. Ogata and S. Hiraoka, *Eur. J. Inorg. Chem.*, 2018, 1192–1197.